International Journal of ChemTech Research
CODEN (USA): IJCRGG ISSN: 0974-4290
Vol.7, No.01, pp 293-301, 2014-2015

Investigation of Structural, Thermal and Magnetic Behaviors of Pristine Barium Carbonate Nanoparticles Synthesized by Chemical Co-Precipitation Method

S. Vadivelan[1]*, J. Bennet[1], N. Victor Jaya[1]

[1]Department of physics, Anna University, Chennai-25, India

Abstract: The pristine $BaCO_3$ (Witherite) nanoparticles were prepared via chemical co-precipitation method. The synthesized materials was sintered in two different calcinations temperatures at 650 ℃ and 750 ℃ and characterized by XRD, VSM, TG-DTA, FT-IR, TEM. From XRD data's, the average crystalline size ranges 34-35 nm and pure orthorhombic phase was found. The VSM technique were explained the M-H loops of $BaCO_3$ powders showed a typical antiferromagnetic behaviors with the superimposed to a diamagnetic signal and also showed no sign of a typical Meissner effect when cooled by liquid nitrogen. Hence it has higher coercivity that will be more suitable for magnetic field memory applications as they can store more magnetic energy. TGA/DTA technique is to find the organic and inorganic content of given material and its basic rule of function is the high precision measurement of weight gain/loss with increasing temperature under inert or reactive atmospheres. FT-IR is used to found the absorption band between 400 to1600 cm^{-1} and also found the stretching vibration of different bond. Nanoscale barium carbonate are formed typically in the diameter range is 100-150 nm is found by TEM.

1. Introduction

$BaCO_3$ (Witherite) is used to producing the optical glass, electric condensers, barium salts, biomaterials, aragonite and also used as a precursor of the producing a ferroelectric materials. The chemical co-precipitation method has many advantages such as good control over the stoichiometry, excellent homogeneous particle distribution, efficient reactivity between components and also lower processing temperature. The nanostructural materials are unique characteristics. So that the nanomaterials are obtained from conventional bulk materials. The nanodevices have good chemical, physical properties and potential applications [4-7]. The application of $BaCO_3$ nanomaterials such as cosmetics, medicine, pigments, catalysis, separation method [1, 2]. The wide applications in industry for producing barium ferrite and barium salts, etc, [3].

The pristine Barium carbonate nanoparticles are prepared by co-precipitation method with various temperatures. The raw materials of the barium nitrite and NH_3 were taken in the required ratio with the water is mixed. The mixture of the raw materials were taken in the beaker then, the beaker is placed in the magnetic stirrer and stirring at 60℃-65℃ up to 2hrs [8]. The prepared dissolved solution is 3 or 4 times is washed in distilled water and ethanol separately because of the dust particles is removed. After that we get pristine barium carbonate in the form of powder particles.

The pure barium carbonate powder particles were dried by 80℃ with the help of hot air oven. After that dried powder particles are collected and grinding up to 2 or 3 hrs. The grinding powders were sintered at 650 ℃ and 750 ℃ respectively. The purpose of sintering to remove the dust particles and unwanted chemical compounds. The sintered powder materials are again grained up to 2 or 3 hrs. After the sintering processes, the pristine barium carbonates nanoparticles are characterized by different characterization. From the XRD pattern, the crystal structure of the nanoparticles is found [9, 10].

2. Experimental

2.1 Preparation of $BaCO_3$ Nanoparticles.

$BaCO_3$ nanoparticles were prepared by chemical co-precipitation method. The precursor of this method is barium nitrate ($Ba(NO_3)_2.6H_2O$). Borax aqueous ($Na_4B_4O\ 10H_2O$) were used as a solvent. The molar ratio of the Barium (II) nitrate and Borax aqueous is (1:0.4) mol and the NH_3 solution dropping until the PH value is 7. 2 hr stirred the given mixture with 65℃-70℃ [8]. 2 or 3 times washed the collecting precipitated with distilled water and ethanol separately. The final stage precipitated materials were dried in an oven at 80° C. The resultant nanoparticles were sintered at 650 ℃ and 750 ℃ respectively.

2.2 Measurements and Characterization

X-ray diffractometer of using Cu-Kα radiation (λ=1.5406 Å) as the source of X-ray to identify the structure of the powder sample. The size of the particles also measured by Scherer's formula t= ($0.9\lambda/\beta\cos\theta_B$)[11]. TGA/DTA technique is to found the organic and inorganic content of given material and its basic rule of function is the high precision measurement of weight gain/loss with increasing temperature under inert or reactive atmospheres. FT-IR is used to found the absorption band between 400 to1600 cm^{-1} and also found the stretching vibration of different bond. nanoscale barium carbonate are formed typically in the diameter range is 100-150 nm is found by TEM. From the VSM technique the magnetic properties also analyzed.

3. Result and discussion

3.1 Structural Studies

The nanoparticles were identified by X-ray powder diffraction (XRD) at room temperature on a PAN analytical X"pert PRO X-ray diffractometer using Cu-Kα radiation (λ=1.5406 Å) for the X-ray source. The crystal structure of the barium carbonate particles is orthorhombic were found by the diffraction peaks of the $BaCo_3$ X-rd pattern (PCPDF #050378). The size of the crystallite is 35-40 nm is calculated by Scherer formula t= ($0.9\lambda/\beta\cos\theta_B$) [1]. Where't' is size of the crystallite, λ is the wavelength of X-ray, B is the full width half maximum of the diffraction peak at θ_B, Where θ_B is known as the diffraction angle. From the Fig. 1. and Fig. 2. We identify the structure is orthorhombic and the lattice parameters are a=5.314, b= 8.904, c=6.430. The experimental and calculate data's are given in table.

Table: 1 The XRD pattern of particles in different crystallography orientation at different sintered temperature

Calcinated temperature T=650°C					
hkl	**2θ**	**d(Å)**	**Intensity**	**FWHM 2θ (deg)**	**D(nm)**
111	24.25	3.68	2997	0.234	35
021	24.85	3.64	1469	0.221	36
221	42.60	2.14	797	0.263	33
Average <t> at 650°C is 34.66 nm					
Calcinated temperature T=750°C					
hkl	**2θ**	**d(Å)**	**Intensity**	**FWHM 2θ (deg)**	**D(nm)**
111	24.25	3.68	3028	0.228	35
021	25.05	3.62	1504	0.200	39
221	42.68	2.13	921	0.272	31
Average <t> at 750°C is 35 nm					

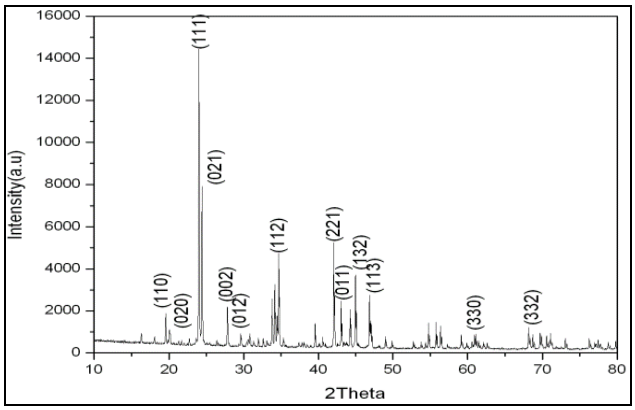

Fig.1. XRD patterns of the $BaCO_3$ nanoparticles calcinated at 650°C with pure orthorhombic phase.

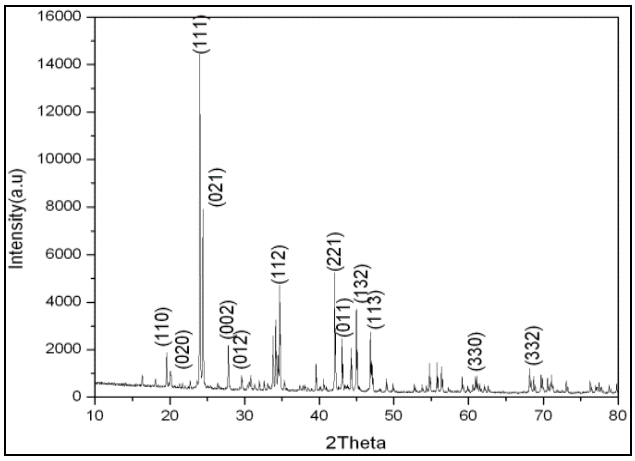

Fig.2. XRD patterns of the $BaCO_3$ nanoparticles calcinated at 750°C with pure orthorhombic phase.

3.2 FT-IR Studies

The FTIR spectrum shows high and low frequency absorption bands corresponding to stretching vibrations. Fig.3a and 3b shows FTIR spectra of $BaCO_3$ recorded in the 400–4000 cm^{-1} wave numbers and strong intensity of the C=H bending vibration indicate at a point is 730 cm^{-1} and 693 cm^{-1}. The C=O symmetric vibration (strong intensity) also indentify the range is 1750 cm^{-1} - 1815 $cm^{-1.}$ C=O stretching vibration indicate the point is 1636 cm^{-1}.

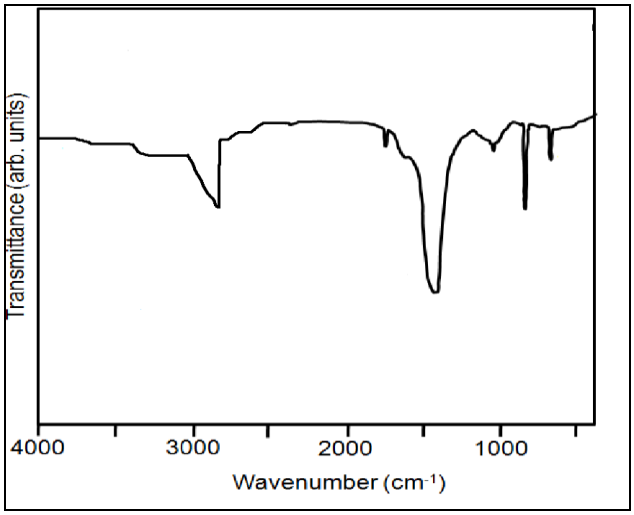

Fig.3a. FT-IR spectrum of $BaCO_3$ Nanoparticles (T=650°C)

In plane and out plane of bending vibration of co_3^{-2} indicate at that point is 693.3 cm^{-1} and 856 cm^{-1}. The metal-oxygen (M-O bond) [14] bending is confirmed by sharp peak at 867.6 cm^{-1}. The absorption bands

were caused by the vibrations in CO_3^{2-} at 400–1800 cm^{-1}. The strong absorption bands for $BaCO_3$ are 1447 cm^{-1} and connected with the asymmetric stretching vibrations. Strong narrow absorption bands at 862 cm^{-1} and 696 cm^{-1} for $BaCO_3$ are assigned to be out of plane bending vibrations and in plane bending vibrations, respectively. Weak narrow absorption bands at 1060 cm^{-1} for $BaCO_3$ due to the symmetric stretching vibrations were detected [15-16]. Due to the covalent bonding of M^{2+} cations (M=Ba) and O^{2-} anions in the $[CO_3]^{2-}$ complexes the cause of changing the efficient masses of the oscillating atomic groups. In addition, O–H stretching and bending vibrations of residual water were detected at 1640 cm^{-1} for $BaCO_3$.

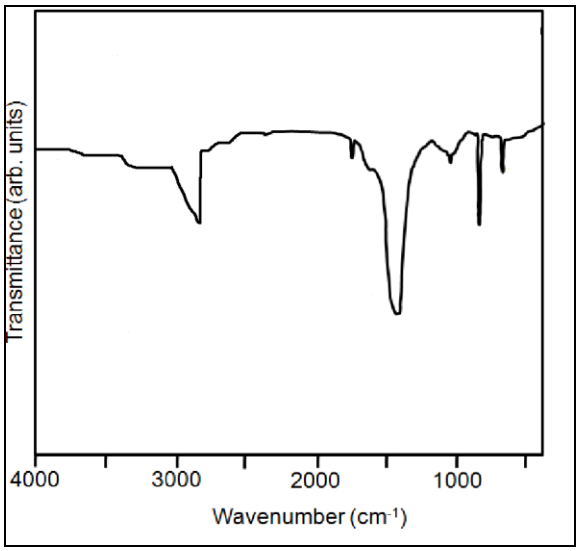

Fig.3b. FT-IR spectrum of $BaCO_3$ Nanoparticles (T=750°C).

3.3 Thermal Studies

TGA is commonly used to determine the characteristics of materials that exhibit either mass loss or gain due to decomposition, oxidation, or loss of elusive (such as moisture) and also found decomposition patterns, studies of degradation mechanisms, reaction kinetics, determination of organic content in a sample, determination of inorganic (e.g. ash) content in a sample. TGA can be used to evaluate the thermal strength of a material. In a desired temperature range, if a species is thermally stable, there will be no observed mass change. Negligible mass loss corresponds to little or no slope in the TGA trace. Beyond this temperature the material will begin to degrade. The small amount of powder sample is characterized by TG-DTA method as shown in fig. 4(a) and 4(b). The spectra can be shown in fig. 4(a) and 4(b), a large endothermic peak and one small shoulder located at 431℃ and 2.71% of mass is loss by vaporization of planar and inner water. The highest sharp exothermal peak at 375.79℃ is drastic loss of mass (≈87%) in the temperature Range is 280℃ – 410℃. The loss of mass due to auto catalytic oxidation and also reduction reaction between the metal nitrates. The broad exothermic peak with the highest at 380℃ is associated only by a small amount of weight loss and there is no loss of mass in the range of temperature 390℃ to 1200℃.

The DSC curve can be used to calculate enthalpies of transitions. This is done by integrating the peak corresponding to a given transition. It can be shown that the enthalpy of transition can be expressed using the following equation

$$\Delta H = KA$$

Where ΔH is the enthalpy of transition, K is the calorimetric constant, and A is the area under the curve. The calorimetric constant will vary from instrument to instrument, and can be determined by analyzing a well-characterized sample with known enthalpies of transition. The DSC curve as shown in Fig. (5a), (5b). The curve shown for $BaCO_3$ exhibits an endothermic peak ~386℃ which confirms transition from cubic to orthorhombic phase of the specimen [20-22]. From these results it is clear that the samples under investigation are in orthorhombic phase at above and room temperature. DSC can also be used to study oxidation, as well as other chemical reactions.

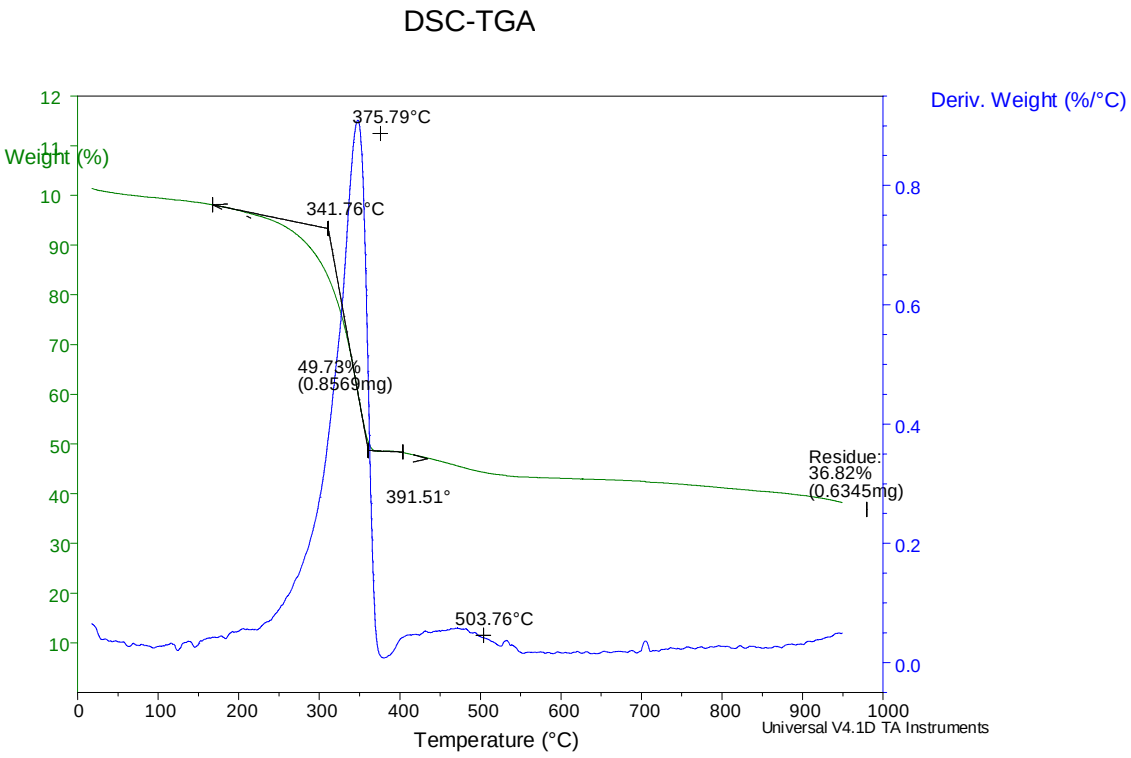

Fig.4a. TG-DTA curves of the $BaCO_3$ Nanoparticles at T=650°C

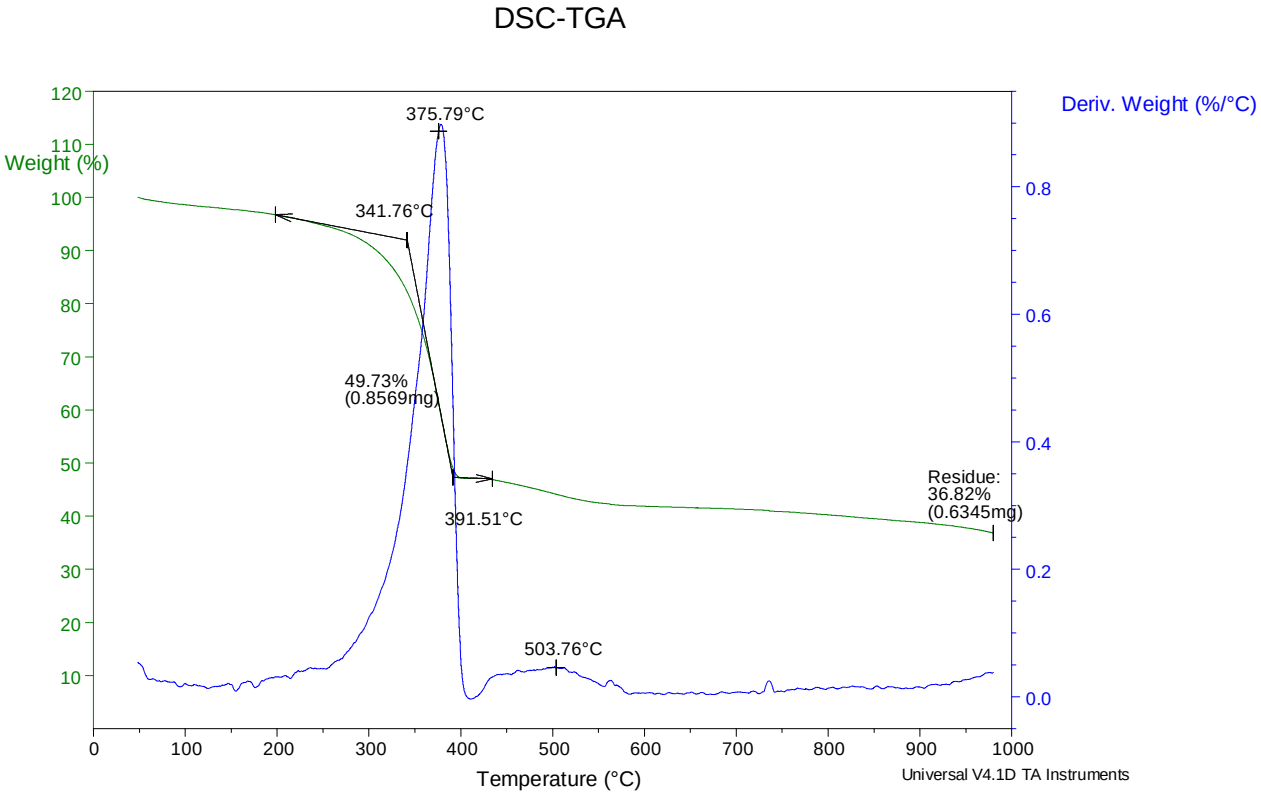

Fig.4b. TG-DTA curves of the $BaCO_3$ Nanoparticles at T=750°C

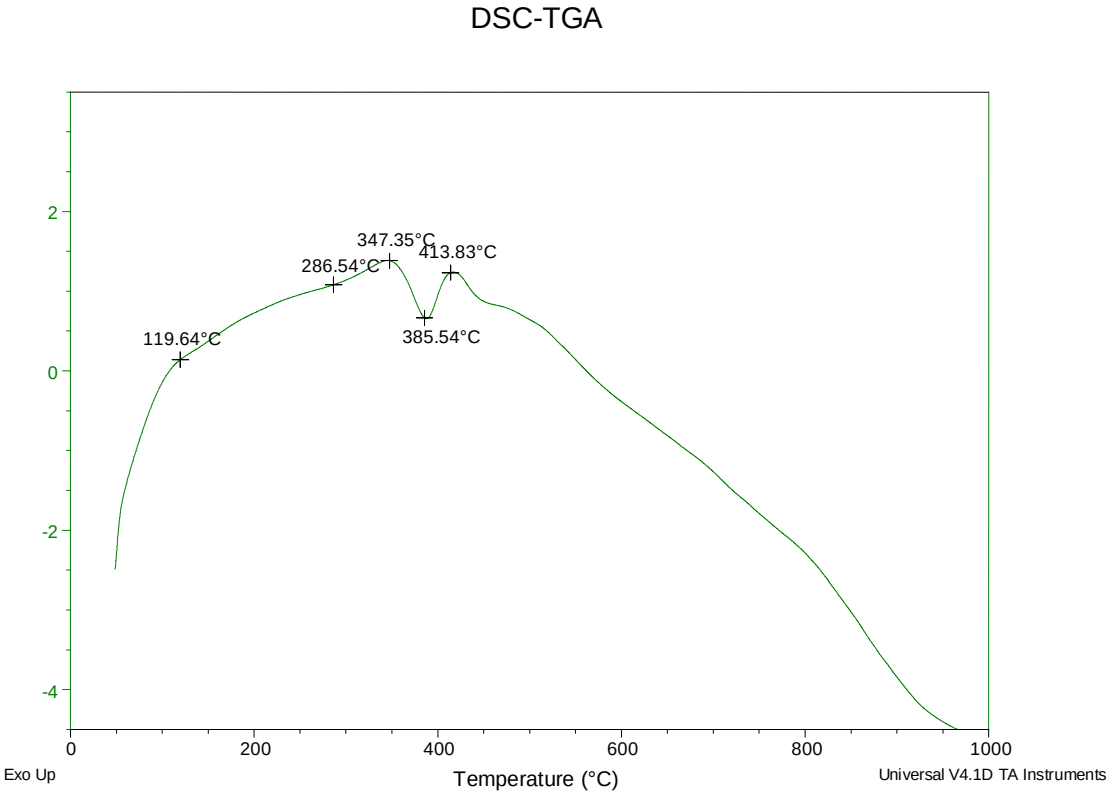

Fig.5a.DSC curves of the $BaCO_3$ Nanoparticles at T=650°C

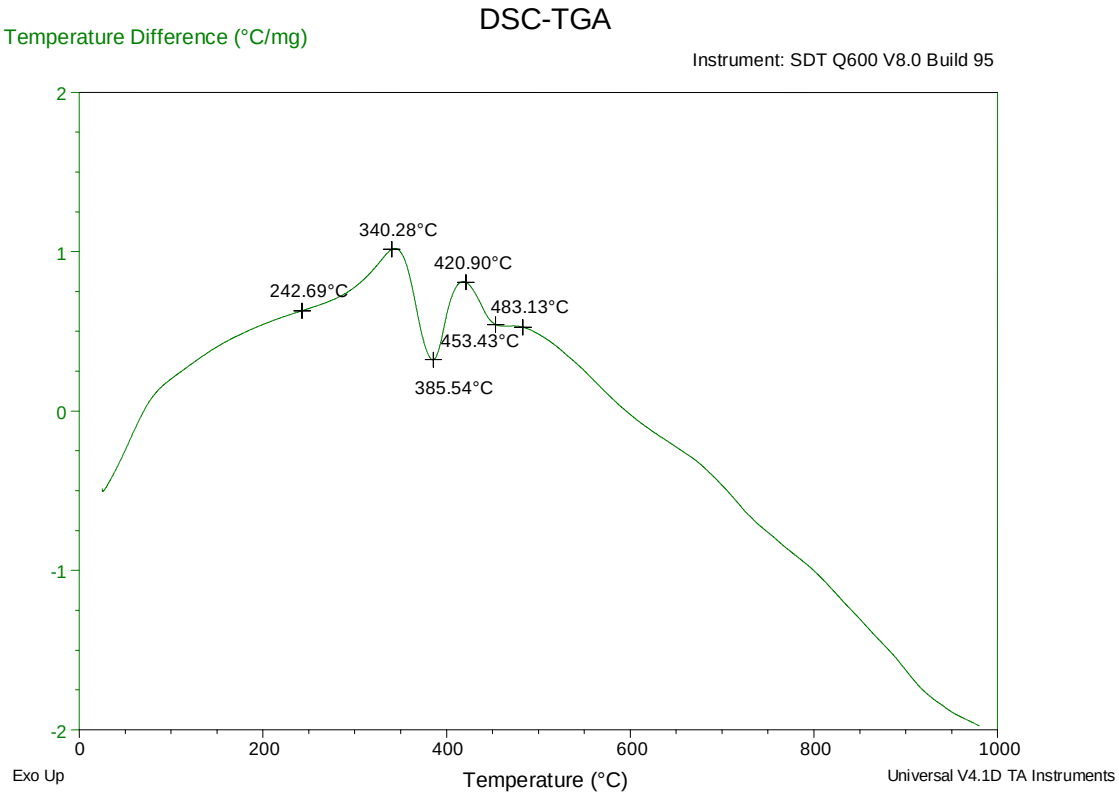

Fig.5b. DSC curves of the $BaCO_3$ Nanoparticles at T=750°C

3.4 Morphology Studies

The TEM microgrant of the $BaCO_3$ nanopowders sintered at T = 650℃ and T = 750 ℃ are shown in Fig. 6a and Fig. 6b. The TEM images of the samples are at sintered at different temperatures and confirmed the

size of the particles in the nanometric range (1-10 nm). It is confirmed from the TEM images that the resultant powders are very small and fine, so the sizes of the particle is less than 10 nm, it is tough to refined the changes between the Fig. 7b and Fig.8b. As it may be we can say erratically the size of the particles increase minute by the increase at the sintered temperature.

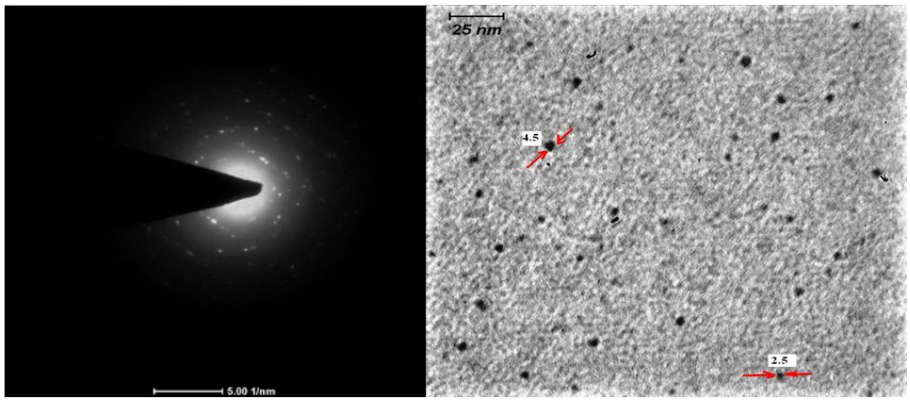

Fig.6a.The TEM image of $BaCO_3$ Nanoparticles at T=650°C

The TEM images results like XRD (Debey Scherer's formula) results confirmed the nanometric sizes of the samples, but TEM shows that the size of the particle range is 1-15 nm[17] and XRD shows that the size of the particle range is 30 nm. The TEM shows the size of the particles and XRD shows the size of the crystallites. Selected area electron diffraction (SAED) pattern (Figs. 7a, 8a) obtained for $BaCO_3$ show a number of spots arranged in circular manner which confirmed the nanocrystalline structure of grown nanoparticles.

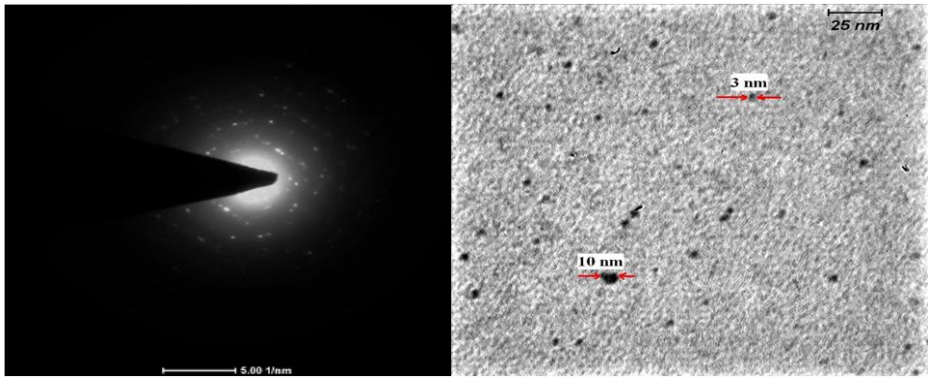

Fig.6a.The TEM image of $BaCO_3$ Nanoparticles at T=750°C

3.5 VSM Studies

In order to determine the magnetic behavior of our samples in more detail, the M-H loops of Sample at room temperature (T = 290K) as shown in Fig. (7a, 7b). It can be clearly seen that the M-H loops indicate the hysteresis typical of ferromagnetic behavior. It is reported that coercivity is closely related to the nature of packing of the grain. The remenance magnetization values of hysteretic loop increased when the milling time increased. The higher coercivity of $BaCO_3$ is due to the increase of magneto crystalline anisotropy and surface anisotropy[18-19]. The coercive force (Hc) and remenant magnetization values were determined at room temperature of the sample to be respectively 88.045 Oe and 0.165 emu/cm^3.

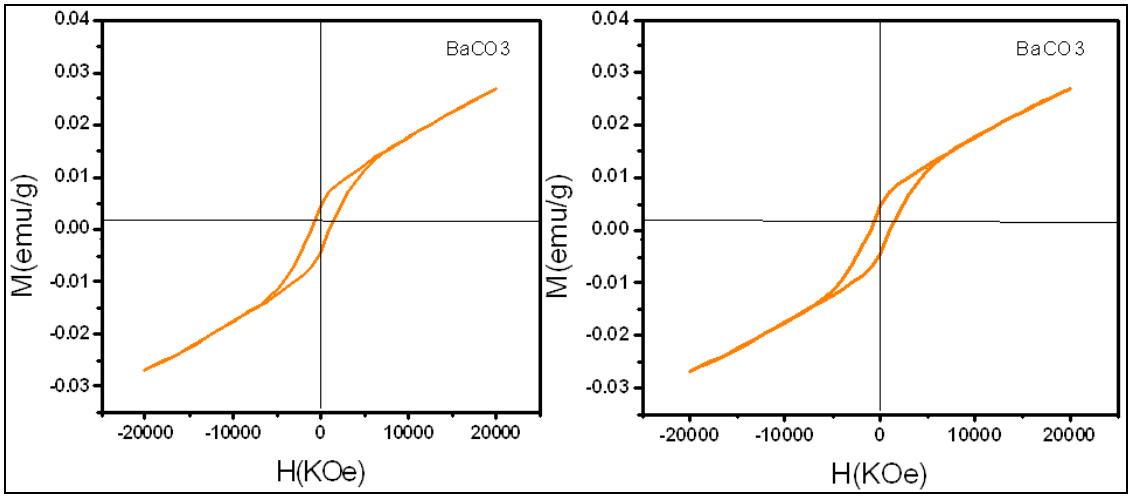

Fig.6a, b.Hysterisis loop of $BaCO_3$ (T=650 °C) and (T=750 °C)

The saturation magnetization of $BaCO_3$ is higher than other compounds. At this point, we decided to find out which compound is responsible for the ferromagnetic character after long grinding times. $BaCO_3$ powders did not show any unusual behavior because of $BaCO_3$ powder was subjected to grinding for 20 hours. Then we measured the M-H loops of the $BaCO_3$ powders showed a typical antiferromagnetic behavior with the superimposed to a diamagnetic signal and also showed no sign of a typical Meissner effect when cooled by liquid nitrogen. Hence it has higher coercivity that will be more suitable for magnetic field memory applications as they can store more magnetic energy.

4. Conclusion

Barium carbonate nanopowders were synthesized by chemical co-precipitation method. From this method the barium carbonate nanoparticle were prepared in two different sintered temperatures T = 650 ℃ and 750 ℃. Nanometric size of the crystallite was confirmed by XRD with debey Scherer's formula. Scherer's formula identify the crystallite sizes about 30 nm and XRD shows that the size in the range of 34-35 nm. The XRD patterns show that the samples sintered at T =650 and 750 ℃ are fully crystallized. The diffraction speaks of the crystallized (shape up) powders compare to each sample allow well with the reflections of pure orthorhombic $BaCO_3$ single phase (witherite) with a = 5.314 Å and b = 8.904 Å. Increase in the sintered temperature decreases the span of the picks, which refers to the augmentation of crystal size and also the concentration of the peaks increase with increasing sintered temperature, which means further crystalline structure. XRD by using of Scherer's formula shows that the mean crystallite sizes increase with the increasing of the sintered temperature, which refers to the more crystalline structure. The vibration modes were studied using FTIR spectroscopy and TGA/DTA can be used to evaluate the thermal stability of a material. In a desired temperature range, if a species is thermally stable, there will be no observed mass change. The morphologies including the particle sizes in nano-scale with good distribution using TEM. Nanometric size of the particles were confirmed by the TEM images of the samples that sintered at T =650 ℃ and T =750 ℃. TEM images show that the sizes of the nanoparticles are in the range of 1-15 nm. This difference of that TEM and XRD is explained that the TEM shows the size of the particles and XRD shows the size of the crystallites. The magnetic studies of VSM were explain the M-H loops of the BaCO3 powders showed a typical antiferromagnetic behavior with the superimposed to a diamagnetic signal and also showed no sign of a typical Meissner effect when cooled by liquid nitrogen. Hence it has higher coercivity that will be more suitable for magnetic field memory applications as they can store more magnetic energy.

References

1. S. H. Yu, and H. Colfen., 2004, Bio-inspired crystal mor-phogenesis by hydrophilic polymers, J. Mater. Chem. 14(14), 2124-2147.
2. H. Colfen, and S. H. Yu., 2005, Biomimetic Mineraliza-tion/Synthesis of Mesoscale Order in Hybrid Inor-ganic–Organic Materials via Nanoparticle Self-Assembly, MRS Bull. 30(10), 727-735.
3. Meshram M.R., Nawal K.A.,Misra P.S., J. Magn. Magn. Mater., 271 (2004), 207-208

4. D. D. Sawall, R. M. Villahermosa, R. A. Lipeles, and A. R. Hopkins., 2004, Interfacial polymerization of polyaniline nanofibers grafted to Au surfaces, Chem. Mater. 16(9), 1606-1608.
5. R. Dewri, and N. Chakraborti. "Simulating recrystallization through cellular automata and genetic algorithms". Modelling Simul. Mater. Sci. Eng. 2005, 13 (3), 173-183.
6. Sa Lv, Ji Sheng, shuang Zhang, Wendong Sun. "Effects of reaction time and citric acid contents on the morphologies of BaCO3 via PVP-assisted method". Material Research Bulletin 43 (2008) 1099-1105.
7. Fangzhi Huanga, Yuhua Shena, Anjian Xiea, , Li Zhangb, Wanghua Xuc, Shikuo Lia and Wensheng Lua. "Polymorph control of a complex $BaCO_3$ superstructure through the cooperation of an insoluble polylactide self-assembled film and soluble poly allylamine modifie", r. Reactive & Functional polymers 69 (2009) 843-850.
8. Sa Lv, Ji Sheng, shuang Zhang, Wendong Sun. "Effects of reaction time and citric acid contents on the morphologies of $BaCO_3$ via PVP-assisted method". Material Research Bulletin 43 (2008), 1099-1105.
9. Sa Lv, Ji Sheng, shuang Zhang, Wendong Sun. "Effects of reaction time and citric acid contents on the morphologies of $BaCO_3$ via PVP-assisted method". Material Research Bulletin 43 (2008), 1099-1105.
10. Fangzhi Huanga, Yuhua Shena, Anjian Xiea, , Li Zhangb, Wanghua Xuc, Shikuo Lia and Wensheng Lua. "Polymorph control of a complex $BaCO_3$ superstructure through the cooperation of an insoluble polylactide self assembled film and soluble poly allylamine modifie", r. Reactive & Functional polymers 69 (2009), 843-850.
11. R. Tholkappiyan, K. Vishista, "N-N-methylene bis acrylamide: A novel fuel for combustion synthesis of zinc ferrite nanoparticles and studied by X-ray photoelectron spectroscopy", International Journal of ChemTech Research 6(5) (2014) 2834-2842.
12. Liu Junliang, Zhang Wei, Guo Cuijing, Zeng Yanwei. "Synthesis and magnetic properties of quasi-single domain M-type barium hexaferrite powders via sol–gel auto-combustion: Effects of pH and the ratio of citric acid to metal ions (CA/M)". Journal of Alloys and Compounds 479 (2009) 863–869.
13. A. Ataie ., S.E. Zojaji. "Synthesis of barium hexaferrite nanoparticles via mechano-combustion route". Journal of Alloys and Compounds 431 (2007) 331–336.
14. Alavi MA, Morsali A. Ultrason Sonochem (2010), 17,132–138.
15. Alavi MA, Morsali A. Ultrason Sonochem (2008), 15, 833–838.
16. Li L, Chu Y, Liu Y, Dong L, Huo L, Yang F. Mater Lett (2006), 60, 2138–2142.
17. Chen L, Shen Y, Xie A, Zhu J, Wu Z, Yang L. Nanosized barium carbonate particles stabilized by cetyltrimethylammonium bromide at the water/hexamethylene interface. Cryst Res Technol 2007; 42: 886.
18. X. Zhang, Y. Duan, H. Guan, S. Liu, B. Wen, J. Magn. Magn. Mater. 310-311 (2007)507.
19. B.A. Jones, M. El-Hilo, K. O'Grady, J. Magn. Magn. Mater. 272–276 (2004) e517
20. R. Kniep, and S. Busch., 1996, Biomimetic growth and self-assembly of fluorapatite aggregates by diffusion into denatured collagen matrices, Angew. Chem., Int. Ed. Engl. 35(22), 2624-2626.
21. S. Busch, H. Dolhaine, A. DuChesne, S. Heinz, O. Hochrein, F. Laeri, O.Podebrad, U. Vietze, T. Weiland, and R. Kniep., 1999, Biomimetic morphogenesis of fluorapatite-gelatin composites: Fractal growth, the question of intrinsic electric fields, core/shell assemblies, hollow spheres and reorganiza-tion of denatured collagen., Eur. J. Inorg. Chem. 1999(10), 1643-1653.
22. S. Sindhu, S. Jegadesan, R. A. Edward Leong, and S. Va-liyaveettil., 2006, Morphosynthesis of mixed metal carbo-nates using micellar aggregation., Crystal Growth & Design. 6(6), 1537-1541.

*****